Non-uniform distribution in μc-Si$_{1-x}$Ge$_x$:H and its influence on thin film and device performance

Yu Cao [a,b], Yiming Liu [a], Jing Zhou [c], Yijun Wang [a], Jian Ni [b], Jianjun Zhang [b,*]

[a] College of Electrical Engineering, Northeast Dianli University, Jilin 132012, China
[b] College of Electronic Information and Optical Engineering, Nankai University, Tianjin 300071, China
[c] College of Chemical Engineering, Northeast Dianli University, Jilin 132012, China

ABSTRACT

In this work, hydrogenated microcrystalline silicon germanium (μc-Si$_{1-x}$Ge$_x$:H) thin films were fabricated by plasma-enhanced chemical vapor deposition (PECVD) and developed as the infrared absorber for thin film silicon solar cells. Three kinds of the non-uniform distribution in μc-Si$_{1-x}$Ge$_x$:H thin films including: "the non-uniform distribution of Si and Ge", the non-uniform distribution of crystallization", and "the non-uniform distribution of H", and how these affect the structural, optical and photoelectric properties of μc-Si$_{1-x}$Ge$_x$:H thin films have been explored. The results show that the good film quality of μc-Si$_{1-x}$Ge$_x$:H is associated with the low crystalline volume fraction and microstructure factor. The band gap of μc-Si$_{1-x}$Ge$_x$:H is determined by the proportion of the Ge-related crystalline networks. In addition, it is suggested that the deterioration of the photosensitivity of μc-Si$_{1-x}$Ge$_x$:H is mainly due to the increase of the Ge clusters with higher micro-void and defect density. Furthermore, by using μc-Si$_{1-x}$Ge$_x$:H bottom sub-cells, the comparable efficiency can be realized under the thin thickness condition. An efficiency of 11.35% in an a-Si:H/a-Si$_{0.6}$Ge$_{0.4}$:H/μc-Si$_{0.5}$Ge$_{0.5}$:H triple junction structure with total cell thickness as thin as 1200 nm was obtained. It is believed that the μc-Si$_{1-x}$Ge$_x$:H thin films can be a better candidate for effective infrared absorber by further improving its microstructure uniformity.

© 2016 Elsevier B.V. All rights reserved.

1. Introduction

Thin film silicon solar cells possess the advantages of low cost, large module area and device flexibility [1]. However, the low conversion efficiency and the light-induced degradation issue have become the obstacles to its development. To get over these drawbacks, multi-junction thin film silicon solar cells, two or more various band-gap sub-cells stack in a vertical manner, have been well documented [2,3]. The world record stabilized efficiency of 13.6% was achieved by Sai et al. with the hydrogenated amorphous silicon (a-Si:H)/ hydrogenated microcrystalline silicon (μc-Si:H)/ μc-Si:H triple junction cell structure [4]. However, although many light management technologies have been used to enhance light trapping [5,6], μc-Si:H solar cell, the conventional bottom sub-cell, has to be thicker than 2 μm due to its low infrared absorption characteristics, leading to a weaker build-in electric field and a longer preparation time, which has several disadvantages for the cell performance and the industrialization process. Nowadays, the quadruple junction thin film silicon solar cells have been realized

[7], which poses much higher requirements on the utilization of the long-wavelength photon energy. Therefore, it is imperative to develop a novel stronger infrared absorber material to meet the demands.

In recent years, μc-Si$_{1-x}$Ge$_x$:H has received attention as an alternative bottom sub-cell absorber for multi-junction thin film silicon solar cells due to its narrower band-gap and higher absorption coefficient than μc-Si:H. In 1998, it was first attempted to use μc-Si$_{1-x}$Ge$_x$:H as the intrinsic layer in the thin film silicon solar cell, this attempt led to the power conversion efficiency of 3.1%, which was, however, a lower efficiency compared to the conventional μc-Si:H solar cell [8]. Then, different source gases e.g., SiH$_4$, Si$_2$H$_6$, GeH$_4$ and GeF$_4$ [9–11], and dilution gases e.g., H$_2$, He and Ar [12–14], were applied to fabricate the μc-Si$_{1-x}$Ge$_x$:H thin films. The structural and photoelectric properties of μc-Si$_{1-x}$Ge$_x$:H thin films were studied carefully [15–21]. Meanwhile, the μc-Si$_{0.9}$Ge$_{0.1}$:H single junction solar cell with conversion efficiency of 8.2% has been obtained [22]. Furthermore, by applying μc-Si$_{1-x}$Ge$_x$:H as the bottom sub-cell absorber, the efficiency of 11.6% [22] and 12.02% [23] has been achieved with the triple junction solar cell structure of a-Si:H/μc-Si:H/μc-Si$_{0.9}$Ge$_{0.1}$:H and a-Si:H/ a-Si$_{0.6}$Ge$_{0.4}$:H/μc-Si$_{0.91}$Ge$_{0.09}$:H respectively. However, the preparation of μc-Si$_{1-x}$Ge$_x$:H is much more complex as different kinds of

* Corresponding author. Tel./fax: +86 22 23508032.
 E-mail address: jjzhang@nankai.edu.cn (J. Zhang).

source gases should be mixed during the deposition. Moreover, the dependence of the material properties on alloy compositions is not well understood in detail.

In this paper, the non-uniform distribution of elements and crystallization in $\mu c\text{-Si}_{1-x}\text{Ge}_x$:H microstructure has been proposed. Based on this, the structural, optical and photoelectric properties of $\mu c\text{-Si}_{1-x}\text{Ge}_x$:H thin films and interrelationships of these characteristics were investigated. Then, $\mu c\text{-Si}_{1-x}\text{Ge}_x$:H was applied as the bottom sub-cell in the triple junction solar cells. The performance of triple junction solar cells with different $\mu c\text{-Si}_{1-x}\text{Ge}_x$:H bottom sub-cells was studied to evaluate its infrared absorption ability.

2. Experimental details

$\mu c\text{-Si}_{1-x}\text{Ge}_x$:H thin films and solar cells were prepared in an in-line seven-chamber RF-PECVD system. The $\mu c\text{-Si}_{1-x}\text{Ge}_x$:H thin films were deposited by gaseous mixtures of H_2, SiH_4 and GeH_4. The RF power, substrate temperature and electrode distance were 30–120 W, 180–260 °C and 7–25 mm, respectively. The concentration of germane GC= $[\text{GeH}_4]/([\text{SiH}_4]+[\text{GeH}_4])$ was in the range 0–100% to obtain various Ge contents. The concentrations of silane and germane $(\text{S}+\text{G})\text{C}=([\text{SiH}_4]+[\text{GeH}_4]) / ([\text{H}_2]+[\text{SiH}_4]+[\text{GeH}_4])$ were in the range 0.3–2.5% to adjust the crystalline volume fraction. $\mu c\text{-Si}_{1-x}\text{Ge}_x$:H thin films were deposited on Eagle 2000 glass substrates, stainless steel plates and crystalline silicon wafers for different measurements. The Ge content x was measured by XRF. The transmission and reflection spectra were measured by UV–vis–NIR spectrophotometer so as to obtain the optical absorption coefficient spectra. The structural properties were studied by Raman spectroscopy using 633 nm laser light and FTIR in the range 400–4000 cm^{-1}. The photoelectric properties were carried out by the coplanar conductivity measurement under dark and AM1.5 (100 mW/cm²) illumination. The triple junction solar cells consist of Glass/SnO₂:F/p-a-SiC:H/i-a-Si:H/n-μc-Si:H/p-a-SiC:H/i-a-Si₀.₆Ge₀.₄:H/n-μc-Si:H/p-μc-Si:H/i-μc-Si$_{1-x}$Ge$_x$:H/n-a-Si:H/ZnO/Ag. The textured SnO₂ (Asahi U type) was applied as the front TCO. The area of the solar cell was 10×10 mm². Current density–voltage (J–V) curve was characterized under AM1.5 conditions at 100 mW/cm². The quantum efficiency (QE) of the individual sub-cells of the triple junction solar cell was determined under bias-light illumination. The corresponding short-circuit current density (J_{sc}) values ($J_{sc.top}$, $J_{sc.mid}$, $J_{sc.bot}$) are calculated from the QE curves, the smallest of which was used as J_{sc} for the solar cell efficiency calculation.

3. Results and discussion

3.1. Non-uniform distribution in $\mu c\text{-Si}_{1-x}\text{Ge}_x$:H

Fig. 1 displays the Raman spectra of $\mu c\text{-Si}_{1-x}\text{Ge}_x$:H thin films with different crystalline volume fractions by adjusting (S+G)C. The Ge content of the film is ~0.6. The spectra are normalized to the highest peak intensities. Three peaks around 500, 400 and 280 cm^{-1} are observed which belong to the Si–Si, Si–Ge and Ge–Ge vibrations respectively [16]. The film exhibits completely amorphous structure with the high (S+G)C of 2%. When the (S+G)C is lower than 1.2%, the Si–Si crystalline peak at 500 cm^{-1} can be detected, indicating that the films become microcrystalline. For the $\mu c\text{-Si}_{1-x}\text{Ge}_x$:H Raman spectra, the amorphous and crystalline peaks of Si–Si, Si–Ge and Ge–Ge are hard to be decomposed because of its complexity. As far as we know, the reports regarding the peak analysis in Raman spectra of $\mu c\text{-Si}_{1-x}\text{Ge}_x$:H thin films are rare. However, as shown in Fig. 1, the Raman spectra of a-Si$_{1-x}$Ge$_x$:H thin
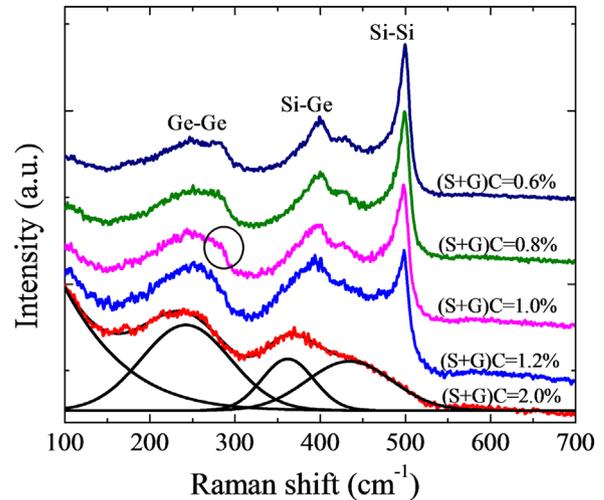
Fig. 1. Raman spectra of $\mu c\text{-Si}_{1-x}\text{Ge}_x$:H thin films with different (S+G)C.

films can be easily decomposed into three Gaussian peaks to determine the contribution of Si–Si, Si–Ge and Ge–Ge bonds [24]. The results of decomposition have been used for calculating the fraction of Si–Ge bonds (F) by

$$F = \frac{I_{Si-Ge}}{I_{Si-Si}+I_{Si-Ge}+I_{Ge-Ge}}, \tag{1}$$

where I_{Si-Si}, I_{Si-Ge} and I_{Ge-Ge} are the integral intensities of Si–Si, Si–Ge and Ge–Ge modes, respectively. For the a-Si₀.₄Ge₀.₆:H thin film in Fig. 1, the F of the experimental structure (F_e) deduced from the Raman spectrum is 0.18.

In order to reduce the band gap of $\mu c\text{-Si}_{1-x}\text{Ge}_x$:H thin films effectively, the Si–Ge bonds in the film network are expected to be as many as possible. The ideal network would be atomic ordering structure, as shown in Fig. 2(a). In this case, the film consists entirely Si–Ge bonds, and the F of atomic ordering structure (F_a) is equal to $2n$ ($n=\min (x, 1-x)$) [25]. However, due to the similarity of the binding energy of Si–Si, Si–Ge and Ge–Ge bonds. The Ge and Si atoms may tend to bond in a random way (Fig. 2(b)). The F of random structure (F_r) is equal to $2x(1-x)$ [26]. The F_a and F_r of a-Si₀.₄Ge₀.₆:H thin films are 0.8 and 0.48 respectively. The F_e is much lower than the F_r, let alone the F_a. This is probably due to the existence of the two-phase separation growth. The Ge radicals have a higher viscosity coefficient and a lower diffusion length compared to the Si radicals. Therefore, the Ge radicals tend to gather together as a cluster with the formation of Ge–Ge bonds, which reduces the proportion of Si–Ge bonds, and also lets the remaining Si radicals gather together to form the Si clusters, resulting in the formation of the Si and Ge clusters in the films, as shown in Fig. 2(c). Due to the similar growth patterns, the growth of $\mu c\text{-Si}_{1-x}\text{Ge}_x$:H is also constituted by the random growth mode and the two-phase separation growth mode. Thus, the microstructure of $\mu c\text{-Si}_{1-x}\text{Ge}_x$:H will contain the Si and Ge clusters, and it also has been confirmed by theoretical simulation [27]. We call this kind of non-uniform as "the non-uniform distribution of Si and Ge" in $\mu c\text{-Si}_{1-x}\text{Ge}_x$:H.

From Fig. 1, it can be found that the crystalline volume fraction of $\mu c\text{-Si}_{1-x}\text{Ge}_x$:H thin films is increased by decreasing the (S+G)C. When the (S+G)C reaches 1.2%, the Si–Si crystalline peak appears; however, no Ge–Ge crystalline peak can be seen in the spectrum which implies that the Ge–Ge network is still amorphous. The Ge–Ge crystalline peak began to appear by further reducing the (S+G)C to 1%. Meanwhile, the Si–Si crystalline peak is quite sharp, indicating a higher crystallinity. Thus the sequence of crystalline volume fraction in $\mu c\text{-Si}_{1-x}\text{Ge}_x$:H films from high to low is: Si–Si network, Si–Ge network and Ge–Ge network. Moreover, from the